

EchoMimicV2: Towards Striking, Simplified, and Semi-Body Human Animation

Rang Meng Xingyu Zhang Yuming Li Chenguang Ma

Terminal Technology Department, Alipay, Ant Group

{mengrang.mr, zxy449919, luoque.lym, chenguang.mcg}@antgroup.com

Project Page: https://antgroup.github.io/ai/echomimic_v2

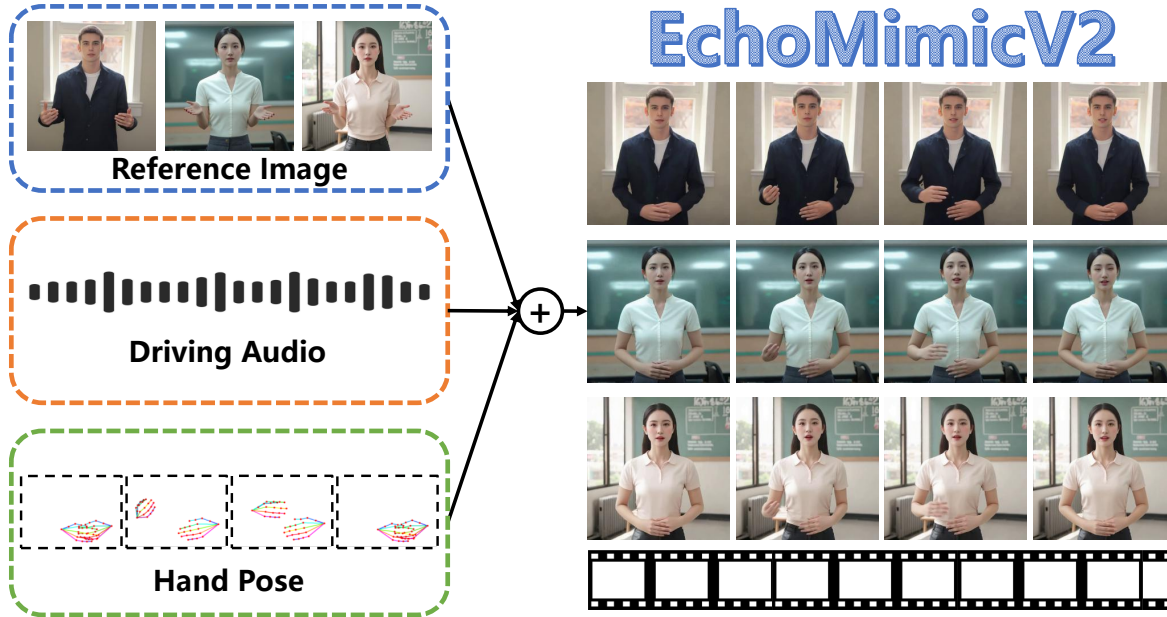


Figure 1. EchoMimicV2 utilizes a reference image, an audio clip, and a sequence of hand pose to generate a high-quality animation video, ensuring coherence between audio content and half-body movements.

Abstract

Recent work on human animation usually involves audio, pose, or movement maps conditions, thereby achieves vivid animation quality. However, these methods often face practical challenges due to extra control conditions, cumbersome condition injection modules, or limitation to head region driving. Hence, we ask if it is possible to achieve striking half-body human animation while simplifying unnecessary conditions. To this end, we propose a half-body human animation method, dubbed **EchoMimicV2**, that leverages a novel **Audio-Pose Dynamic Harmonization** strategy, including **Pose Sampling** and **Audio Diffusion**, to enhance half-body details, facial and gestural expressiveness, and meanwhile reduce conditions redundancy. To compensate for the scarcity of half-body data, we utilize **Head Partial Attention** to seamlessly accommodate head-shot data into our training framework, which can be omit-

ted during inference, providing a free lunch for animation. Furthermore, we design the **Phase-specific Denoising Loss** to guide motion, detail, and low-level quality for animation in specific phases, respectively. Besides, we also present a novel benchmark for evaluating the effectiveness of half-body human animation. Extensive experiments and analyses demonstrate that EchoMimicV2 surpasses existing methods in both quantitative and qualitative evaluations.

1. Introduction

Diffusion-based video generation has seen significant advancements[1, 3, 5, 8, 8, 9, 11, 12, 12, 21, 21, 33], prompting extensive research in human animation. Human animation, as a subset of video generation domain, aims at synthesizing natural and realistic human-centric video sequences from a reference character images. Current research on human animation commonly employs pre-trained diffusion models as backbone, and involves cor-

responding condition injection modules to introduce control conditions[6, 14, 17, 26, 30, 31, 37, 38], so that life-like animation can be well generated. Unfortunately, there is still gaps between academic study and industrial needs: 1) Head region limitation; 2) Condition-injection complexity. 1) **Head Region Limitation**. On the one hand, prior human animation works[6, 30, 31, 37] mainly focus on generating head-region videos, neglecting the synchronization of the audio and the shoulders-below body. The most recent work[17] has improved half-body animation with auxiliary conditions and injection modules beyond audio-driven module. 2) **Condition-Injection Complexity**. On the other hand, the commonly-used control conditions (*e.g.* text, audio, pose, optical flow, movement maps) can provide a solid foundation for lifelike animation. Particularly, current research efforts concentrate on aggregating supplementary conditions, which result in unstable training due to multi-condition incoordination, and elevated inference latency stemming from intricate condition-injection modules.

For the first challenge, a straightforward baseline exists to accumulate conditions related to shoulder-below body, such as half-body key points maps. However, we discover that this approach remains infeasible because of increased complexity of conditions (for the second challenge).

In this paper, to remedy the aforementioned issues, we introduce an novel end-to-end method-EchoMimicV2, building upon the portrait animation method EchoMimic [6]. Our proposed EchoMimicV2 strives for striking quality of half-body animation yet with simplified conditions. To this end, EchoMimicV2 exploits the Audio-Pose Dynamic Harmonization (APDH) training strategy to modulate both audio and pose conditions, and meanwhile reduce the redundancy of the pose condition. Additionally, it utilizes a stable training objective function, termed Phase-specific Loss (PhD Loss), to enhance motion, details, and low-level quality, replacing the guidance of redundant conditions.

Specifically, APDH is inspired by the waltz dance step, where audio and pose condition perform as synchronized dance partners. As the pose gracefully steps back, the audio seamlessly advances, perfectly filling in the space to create a harmonious melody. As a result, the control scope of the audio condition is extended from the mouth to the entire body via Audio Diffusion, and meanwhile the pose condition is confined from the entire body to the hands via Pose Sampling. Given that the primary regions responsible for audio expression located in the mouth lips, we initiate our audio condition diffusion from the mouth part. Additionally, due to the complementarity of gestural and verbal communication, we retain hand pose condition for the gesture animation so that the Head Region Limitation challenge is overcome, extending to half-body region animation.

Throughout this process, we find a free lunch for data augmentation. When audio condition only controls the head

EchoMimicV2	CyberHost[17]
Audio+RefImage	
+ Hand Pose Sequence	+ Body Movement Sequence
-	+ Face Crop Injection Module
-	+ Hand Crop Injection Module
-	+ Full-body Pose Guidance

Table 1. The simplification of our proposed EchoMimicV2.

region via Head Partial Attention, we can seamlessly incorporate padded headshots data to enhance facial expressions without requiring additional plugins like[17]. We also list the advantages of our proposed EchoMimicV2 in Table 1.

Moreover, we propose a stable training objective function, Phase-specific Loss (PhD Loss), with two goals: 1) to enhance the motion representation with incomplete pose; 2) to improve details and low-level visual quality not governed by audio. While it is intuitive to employ a multi-loss mechanism that integrates pose, detail, and low-level visual objective functions concurrently, such an approach typically requires extra models, including Pose Encoders and VAE Decoders. Given that the ReferenceNet-based backbone already demands significant computational resources[14], implementing a multi-losses training becomes impractical. Through experimental analysis, we segments the denoising process into three distinct phases, each with its primary focus: 1) Pose-dominant phase, where motion poses and human contours are initially learned; 2) Detail-dominant phase, where character-specific details are refined; and 3) Quality-dominant phase, where the model enhances the color and other low-level visual qualities. Consequently, the proposed PhD Loss is tailored to optimize the model for each specific denoising phase, that is, Pose-dominant Loss for the early phase, Detail-dominant Loss for the middle phase, and Low-level Loss for the final phase, ensuring a more efficient and stable training process.

Additionally, to facilitate the community in quantitative evaluation of half-body human animation, we have curated a test benchmark, named EMTD, comprising half-body human videos sourced from the Internet. We conducted extensive qualitative and quantitative experiments and analyses, demonstrating that our method achieves state-of-the-art results. In summary, our contributions are as follows:

- We propose EchoMimicV2, an end-to-end audio-driven framework to generate striking half-body human animation yet driven by simplified conditions;
- We propose APDH strategy to meticulously modulate audio and pose condition, and reduce pose condition redundancy;
- We propose HPA, a seamlessly data augmentation to enhance the facial expressions in half-body animations, no need for additional modules;
- We propose PhD Loss, a novel objective function to enhance the motion representation, appearance details and low-level visual quality, alternating the guidance of com-

plete pose condition;

- We provide a novel evaluation benchmark for half-body human animation.
- Extensive experiments and analyses are conducted to verify the effectiveness of our proposed framework, which surpasses other state-of-the-arts methods.

2. Related Work

2.1. Pose Driven Human Animation

Many human animation methods focus on pose-driven settings, using pose sequences from driving video. Research in pose-driven human video generation typically follows a standard pipeline, employing various pose types, such as skeleton pose, dense pose, depth, mesh, and optical flow—as guiding modalities, alongside text and speech inputs. Conditional generation models have advanced with stable diffusion (SD) or Stable Video Diffusion (SVD) as their backbone. Methods like MagicPose[4] integrate pose features into diffusion models via ControlNet[36], while methods like AnimateAnyone[14], MimicMotion[38], MotionFollower[24], and UniAnimate[27] extract skeleton poses using DWPose[35] or OpenPose[20]. These methods use lightweight neural networks with a few convolutional layers as pose guides to align skeleton poses with latent space noise during denoising. In contrast, DreamPose[15] and MagicAnimate[32] use DensePose[10] to extract dense pose information, which is concatenated with noise and input into the denoising UNet by ControlNet[36]. Human4DiT[22], inspired by Sora, extracts 3D mesh maps using SMPL[2] and adopts the Diffusion Transformer for video generation.

2.2. Audio Driven Human Animation

The goal of audio-driven human animation is to generate gestures from speech audio, ensuring motion aligns with audio in semantics, emotion, and rhythm. Existing works often focus on talking heads. EMO[23] introduces a Frame Encoding module for consistency. AniPortrait[30] advances 3D facial structures mapped to 2D poses for coherent sequences. V-Express synchronizes audio with lip movements and expressions, refining emotional nuances. Hallo[31] uses diffusion models for enhanced control over expressions and poses. Vlogger[39] generates talking videos from a single image via a diffusion model for high-quality, controllable output. MegActor- Σ [34] integrates audio and visual signals into portrait animation with a conditional diffusion transformer. TANGO[18] generates co-speech body-gesture videos, improving alignment and reducing artifacts. Additionally, EchoMimic[6] is capable of generating portrait videos not only by audios and facial pose individually, but also by a combination of both audios and selected facial pose. CyberHost[17] supports combined control signals

from multiple modalities, including audio,full-body keypoints map, 2D hand pose sequence, and body movement maps.

3. Method

3.1. Preliminaries

Latent Diffusion Model. Our approach builds upon the Latent Diffusion Model (LDM)[21], which employs a Variational Autoencoder (VAE) Encoder[16] E to map an image I from the pixel space to a more compact latent space, represented as $z_0 = E(I)$. During training, Gaussian noise is progressively added to z_0 across various timesteps $t \in [1, \dots, T]$, ensuring that the final latent representation z_T follows a standard normal distribution $\mathcal{N}(0, 1)$. The primary training objective of LDM is to estimate the noise introduced at each timestep t ,

$$L_{latent} = \mathbb{E}_{z_t, t, c, \epsilon \sim \mathcal{N}(0, 1)} [\|\epsilon - \epsilon_\theta(z_t, t, c)\|_2^2] \quad (1)$$

where ϵ_θ represents the trainable Denoising U-Net, and c denotes the conditions like audio or text. During the inference phase, the pretrained model is used to iteratively denoise a latent vector sampled from a Gaussian distribution. The denoised latent is subsequently decoded back to an image using the VAE Decoder D .

ReferenceNet-based Backbone. As EchoMimic[6] and other prevalent portrait animation work[30, 31, 37], we exploit the ReferenceNet-based diffusion architecture as our backbone. In the ReferenceNet-based backbone, we utilize a duplicate of the pretrained 2D U-Net as the ReferenceNet to extract reference features from the reference images. These features are then injected into the Denoise U-Net through cross-attention mechanisms to maintain appearance consistency between the generated images and the reference image. Additionally, we utilize a pretrained Wav2Vec model as the Audio Encoder E_A to extract audio embeddings, and then inject as the audio condition c_a via Audio Cross Attention blocks in the Denoising U-Net, for the synchronization between motion and audio. Besides, we also integrate a Pose Encoder E_p to extract keypoint maps. These keypoint maps are then concatenated with the noise latents and fed into the Denoise U-Net, serving as pose condition. Finally, we inject Temporal-Attention blocks into Denoise U-Net to capture inter-frame motion dependencies, for motion smoothness of the animation.

3.2. Audio-Pose Dynamic Harmonization

In this section we introduce the core training strategy of EchoMimicV2, Audio-Pose Dynamic Harmonization (APDH). APDH is exploit to progressively reduce the condition complexity and modulate the audio and pose condition in a waltz step-like manner. This strategy consists of two main components: Pose Sampling (PS) and Audio Diffusion (AD).

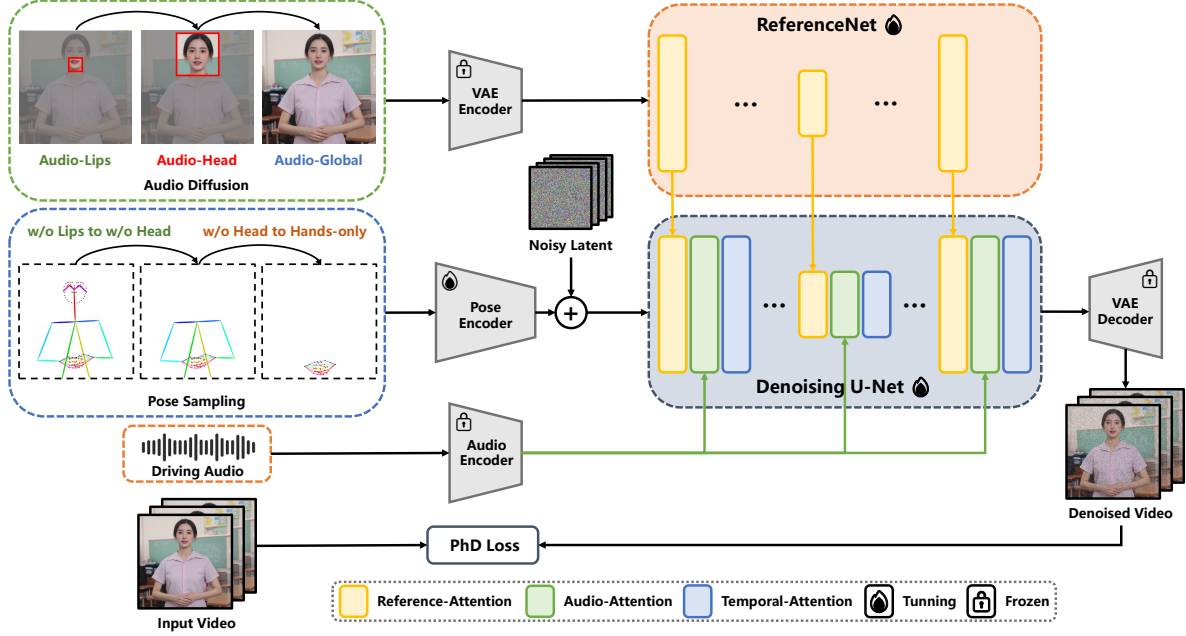


Figure 2. The overall pipeline of our proposed EchoMimicV2.

3.2.1. Pose Sampling

Initial Pose Phase. We start the training of our framework with a complete pose-driven stage. Let \mathcal{P}^{init} represent the complete key points maps of the half-body human figures, encoded by a Pose Encoder E_P . During this stage, we mute the Audio Cross Attention blocks and only optimize other modules in the Denoising U-Net to provide a comprehensive recognition of the human actions.

Iterative Pose Sampling Phase. At the iteration level, we progressively sample some iteration steps for pose condition dropout with a iteration-increasing probability. This gradual dropout helps to mitigate over-reliance on the pose condition.

Spatial Pose Sampling Phase. At the spatial level, we sample pose condition by removing key points as the following order: the lips part first, the head second, and the body part finally. We denote the sampled pose conditions as \mathcal{P}^{-lips} , \mathcal{P}^{-head} , and \mathcal{P}^{hands} , respectively. By doing so, the control of the pose condition over lip movements, facial expressions, and body (respiratory rhythms) are diminished in a step-by-step manner, thereby creating space for audio-driven procedure, allowing the audio condition to play a dominant role.

3.2.2. Audio Diffusion

In the Initial Pose and Interactive Level Pose Sampling phase, the Audio Cross-Attention blocks are completely frozen. In the Spatial Level Pose Sampling phase, audio condition begins to be integrated progressively.

Audio-Lips Synchronization. After removing keypoints of lips, spatial mask \mathcal{A}_{lips} for lips is applied on Audio Cross-

Attention blocks as Lips Partial Attention, forcing audio condition solely controlling the lips movements. By doing so, audio-lips synchronization is enhanced.

Audio-Face Synchronization. After removing keypoints of head, the spatial mask \mathcal{A}_{lips} is diffused to a head part as \mathcal{A}_{head} , and is applied to Audio Cross-Attention blocks as Head Partial Attention. This allows the audio condition to dominate the overall facial expression, enhancing audio-face expression synchronization.

Audio-Body Correlation. With the hands-only keypoints \mathcal{P}^{hands} , partial mask is diffused to the global space. This results in an entirely audio-driven half-body animation, accompanied by a pose emphasis on the hands. Note that the hands part serve as intersection between audio and pose condition. Thus, more audio cues are translated into appropriate gestures, allowing for a better capture of audio-gesture correlation.

3.3. Head Partial Attention for Data Augmentation

During Audio-Face Synchronization, we introduce head-shot data to offset the scarcity of half-body data and enhance facial expression. To achieve this, we pad the headshot data to strictly align the spatial dimensions and head location of half-body images. And then we reuse the Head Partial Attention to exclude the padded parts as shown in Figure 2. Notably, no additional cross-attention blocks are required. To mitigate the impact of the padding for source distribution, we incorporate this step before introducing half-body data in the Audio-Face Synchronization phase.



Figure 3. The results of EchoMimicV2 given different reference images, hand pose and audios.

3.4. Temporal Modules Optimization

Following the EchoMimic[6], we integrate Temporal Cross Attention blocks into the Denoising U-Net and initialize its weights using EchoMimic. During the optimization of the Temporal modules, we use 24-frame video clips as input and freeze the other modules to ensure stability.

3.5. Phase-specific Denoising Loss

Besides the aforementioned condition design and training strategy, we also improve performance via the Phase-specific Denoising Loss (PhD Loss) L_{PhD} . We divide the multi-timestep denoising process into three phases based on their primary tasks: 1) Pose-dominant phase (early) \mathcal{S}_1 ; 2) Detail-dominant phase (middle) \mathcal{S}_2 ; 3) Quality-dominant phase (final) \mathcal{S}_3 . Accordingly, L_{PhD} includes three tailored losses, denoted as Pose-dominant Loss L_{pose} , Detail-dominant Loss L_{detail} , and Low-level Loss L_{low} , which are applied sequentially across these three phases.

Pose-dominant Loss L_{pose} : Specifically, we first adopt one-step sampling to calculate the prediction Z_0^t for the latent output Z_t of timestep t from Denoising U-Net. And then, we decode the latent Z_0^{pred} by VAE decoder D , to obtain the RGB form I_0^t for Z_t . Next, we employ the Pose Encoder E_P to extract the keypoints map of I_0^t and the target image I_{target} as \mathcal{M}_0^t and \mathcal{M}_{target} , respectively. Finally, we implement MSE loss on the \mathcal{M}_p^t and \mathcal{M}_p^{target} to calculate

the L_{pose} in \mathcal{S}_1 as follow:

$$L_{pose} = MSE(\mathcal{M}_p^t, \mathcal{M}_p^{target}) \quad (2)$$

Detail-dominant Loss L_{detail} : We use a Canny operator as used in ControlNet[36] to extract the edges and other high-frequency details of I_0^t and I_{target} as \mathcal{M}_d^t and \mathcal{M}_d^{target} , respectively. And then we calculate the MSE loss of \mathcal{M}_d^t and \mathcal{M}_d^{target} as the L_{detail} in \mathcal{S}_2 :

$$L_{detail} = MSE(\mathcal{M}_d^t, \mathcal{M}_d^{target}) \quad (3)$$

Low-level Loss L_{low} : We exploit LPIPS following the Spatial Loss of EchoMimic as our L_{low} in \mathcal{S}_3 :

$$L_{detail} = LPIPS(I_0^t, I_{target}) \quad (4)$$

We also follow the latent loss in LDM to optimize the model, denoted as L_{latent} . An then we obtain the overall PhD Loss as follows:

$$L_{PhD} = \begin{cases} \lambda_{pose} \cdot L_{pose} + L_{latent} & t \in \mathcal{S}_1 \\ \lambda_{detail} \cdot L_{detail} + L_{latent} & t \in \mathcal{S}_2 \\ \lambda_{low} \cdot L_{low} + L_{latent} & t \in \mathcal{S}_3 \end{cases} \quad (5)$$

where λ_{pose} , λ_{detail} , and λ_{low} is the loss weights.

4. Experiments

In this section, we first provide the implementation details, training datasets, evaluation benchmarks used in our exper-

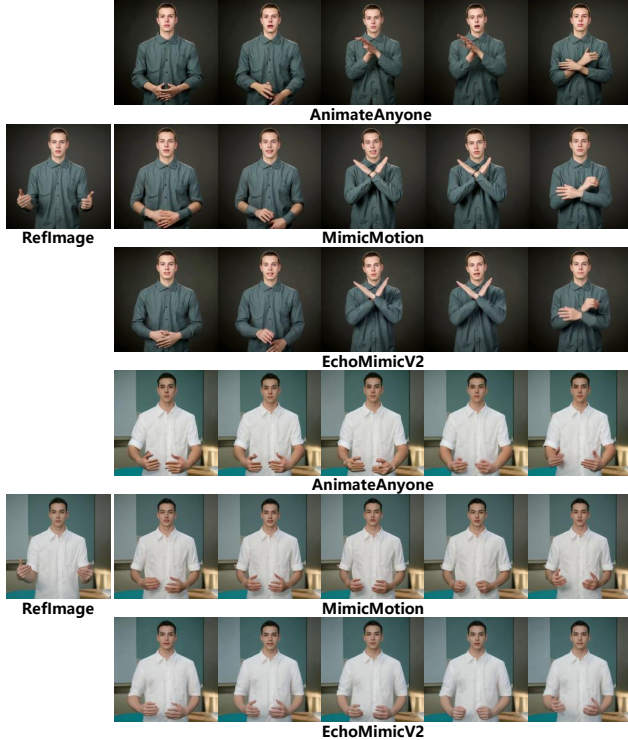


Figure 4. The results of EchoMimicV2 compared to pose-driven half-body human animation baselines.

iments. Following this, we evaluate the superior performance of our approach via quantitative and qualitative comparisons with comparable methods. Next, we also perform ablation studies to analyze the effectiveness of each component of our method.

4.1. Experimental Setups

Implementation Details. Our training procedure includes two stages. In the first stage, the model is trained to generate target frames from reference images, ensuring visual consistency. We first employ complete key points maps \mathcal{P}^{init} as pose condition to train the Pose Encoder and Denoising U-Net jointly, while Audio Cross Attention is masked. This process is conducted on 8 A100 GPUs for 10,000 iterations, with a batch size of 4 and a resolution of 768×768 per GPU. And then we train our framework with Audio-Pose Dynamic Harmonization. We train our framework for 10,000 steps in the Iterative Pose Sampling Phase, with the dropout probability for pose condition increasing from 0% to 20%. In the Spatial Pose Sampling Phase, we first train our framework by 10,000 steps utilizing \mathcal{P}^{-lips} and Lips Partial Attention, and then train our framework by 10,000 steps with \mathcal{P}^{-head} and Head Partial Attention on headshot data from EchoMimic. Subsequently, we train our framework by 10,000 iterations using half-body data. Finally, we conduct 10,000 iterations with \mathcal{P}^{hands} and global Audio Cross Attention. For the L_{PhD} , the scope of \mathcal{S}_1 is the

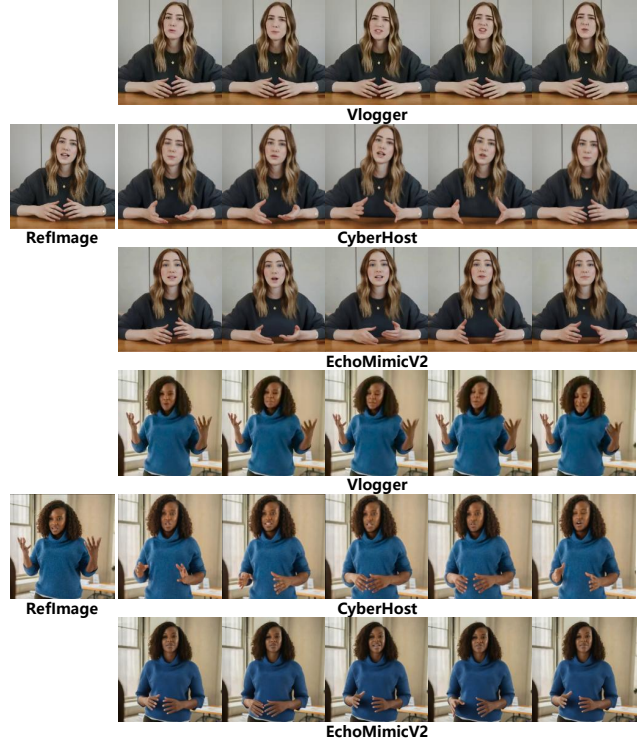


Figure 5. The results of EchoMimicV2 compared to audio-driven half-body human animation baselines.

early 10% timesteps, the scope of \mathcal{S}_2 is the following 60% timesteps, and the rest timesteps is divided into \mathcal{S}_3 . And the loss weights of λ_{pose} , λ_{detail} , and λ_{low} is all set to 0.1. In the second stage, we solely optimize the Temporal-Attention modules and other modules frozen with a batch size of 4 for 30,000 steps. For both stages, the learning rate is set to $1e^{-5}$, and the classifier-free guidance (CFG) scale for reference images and audio is set to 2.5.

Training Datasets. Our training dataset comprises three parts: fully pose-driven dataset, half-body dataset, and headshot dataset. We use HumanVid[29] as the fully pose-driven dataset, which includes about 20,000 high-quality human-centric videos with 2D pose annotations. The half-body training dataset is curated from internet videos and focuses on half-body speaking scenarios. This dataset spans 160 hours and includes over 10,000 identities. The headshot dataset is derived from the training dataset used in EchoMimic including 540 hours of talking head videos.

Novel Half-Body Evaluation Benchmark. Public datasets typically evaluate audio-driven talking head or pose-driven human animation, but none specifically target audio-driven half-body animation. To fill this gap, we introduce the EchoMimicV2 Testing Dataset (EMTD) for evaluating half-body human animation. EMTD includes 65 high-definition TED videos (1080P) from YouTube, featuring 110 annotated, clear, and front-facing half-body speech segments. The open-source project will provide scripts for download-

Methods	FID↓	FVD↓	SSIM↑	PSNR↑	E-FID↓	Sync-D↓	Sync-C↑	HKC↑	HKV↑	CSIM↑
AnimateAnyone[14]	58.98	1016.47	0.729	20.579	3.784	13.887	0.987	0.809	23.87	0.387
MimicMotion[38]	53.47	622.62	0.702	19.278	2.628	7.958	1.495	0.907	24.82	0.526
EchoMimicV2	49.33	598.45	0.738	21.986	2.218	7.021	7.219	0.923	25.28	0.558
w/o Initial Pose	49.99	602.08	0.730	21.708	2.235	6.976	7.019	0.873	23.97	0.550
w/o Iterative Pose Sampl.	50.01	605.29	0.727	21.276	2.276	6.987	7.005	0.917	25.24	0.527
w/o Spatial Pose Sampl.	49.39	593.98	0.740	21.994	2.208	7.023	7.220	0.922	25.25	0.532
w/o Headshot Data Aug.	51.29	610.87	0.711	20.965	2.961	6.792	6.394	0.921	25.27	0.527
w/o Audio-Lips Sync.	49.37	599.82	0.722	21.988	2.629	6.803	6.463	0.919	25.24	0.512
w/o Audio-Face Sync.	51.11	620.75	0.719	21.837	2.983	6.807	6.286	0.922	25.26	0.518
w/o Audio-Body Corr.	50.36	603.84	0.733	21.980	2.217	7.025	7.226	0.906	24.98	0.541
w/o L_{pose}	51.30	620.27	0.695	20.783	2.766	6.954	7.063	0.874	22.83	0.549
w/o L_{detail}	51.61	623.56	0.689	20.038	2.904	6.807	6.985	0.896	24.37	0.541
w/o L_{low}	50.86	602.31	0.675	19.786	2.226	7.028	7.223	0.913	25.20	0.547
Straightforward Baseline	51.53	624.98	0.664	19.269	2.779	7.208	6.706	0.825	22.57	0.508

Table 2. Quantitative comparison and ablation study of our proposed EchoMimicV2 and other SOTA methods.

ing, slicing, and processing these videos for evaluation. Due to limited authorization, we only provide qualitative results and won’t display visualization results. We also release characters for reference images, generated by the FLUX.1-dev¹. These resources support comparative experiments and facilitate further research and application.

Evaluation Metric. Half-body human animation methods are evaluated using metrics such as FID, FVD[25], PSNR[13], SSIM[28], E-FID[7]. FID, FVD, SSIM and PSNR is the metrics to evaluate the low-level visual quality. E-FID assesses image authenticity using Inception network features, extracting expression parameters with a face reconstruction method and calculating their FID scores to gauge expression disparities. To evaluate the identity consistency, we calculate the cosine similarity (CSIM) between the facial features of the reference image and the generated video frames. Besides, we also use the SyncNet[19] to calculate Sync-C and Sync-D for valid the audio-lip synchronization accuracy. Additionally, to evaluate the hands parts animation, HKC (Hand Keypoint Confidence) averages is adopted to evaluate hand quality in audio-driven scenarios, and HKV (Hand Keypoint Variance) is calculated to indicate the richness of hand movements.

4.2. Qualitative Results

In order to assess the qualitative results of our proposed EchoMimicV2, we use the FLUX.1-dev generate reference images, and then conduct half-body animation based on these reference images. Our approach generates high resolution half-body human videos using an audio signal, a reference image and a hand pose sequence. Figure 3 showcases the adaptability and resilience of our method in synthesizing a wide range of audio visual outputs with seamless synchronization to the accompanying audio. These results affirm its potential for advancing the state-of-the-art in

audio-driven half-body human video generation, and illustrate that our proposed EchoMimicV2 can be well generalized across diverse characters and intricate gestures.

Comparisons with Pose-Driven Body Methods. We conduct the qualitative evaluation of EchoMimicV2 and compare with state-of-the-art pose-driven methods, including AnimateAnyone[14] and MimicMotion[38], as shown in Figure 5. We can see that our proposed EchoMimicV2 outperforms the current state-of-the-art results in terms of structural integrity and identity consistency, particularly in local regions such as the hands and face. Additional video comparison results can be available in supplement material.

Comparisons with Audio-Driven Body Methods. Only few works, such as Vlogger[39] and CyberHost[17], support audio-driven half-body human animation. Regrettably, these methods have not been open-sourced, posing challenges for direct comparisons. We obtained relevant experimental results from the homepages of these two projects and conducted experiments using the same reference image. As depicted in Figure 4, our proposed EchoMimicV2 surpasses Vlogger and CyberHost in both generated image quality and the naturalness of movements.

4.3. Quantitative Results

As illustrated in Table 2, we quantitatively compare EchoMimicV2 with state-of-the-art human animation methods, including AnimateAnyone[14] and MimicMotion[38]. The results demonstrate that EchoMimicV2 significantly improves overall performance. Specifically, EchoMimicV2 shows substantial enhancements in quality metrics (FID, FVD, SSIM, and PSNR) and competitive results in synchronization metrics (Sync-C and Sync-D). Additionally, EchoMimicV2 surpasses other SOTA methods in the consistency metric (CSIM). Note that EchoMimicV2 achieves a new SOTA in hand related quality metrics (HKV, HKC).

¹<https://github.com/black-forest-labs/flux>

4.4. Ablation Study

We analyze the effectiveness of our Audio-Pose Dynamic Harmonization (APDH) strategy, condition simplifying design and PhD Loss in Table 2.

Analysis for Pose Sampling. We conduct ablation studies to validate the effectiveness of each phase of Pose Sampling. Specifically, we can observe that Initial Pose and Iterative Pose Sampling phase contribute to overall performance improvement, due to the strong motion prior provided by the full-body pose condition. On the other hand, the row 7 of Table 2 shows that complete pose condition (without Spatial Pose Sampling) has limited impact on each metric, indicating the redundancy of full-body pose, and our APDH strategy can still achieve stable animation with hands-only pose condition.

Analysis for Audio Diffusion. As shown in Table 2, the rows 9 and 10 indicate that Audio Diffusion enhances lip movements and facial expressiveness. Furthermore, row 10 demonstrates that the audio condition also improves body and hand animation, indicating that EchoMimicV2 captures the fine-grained correlation, that is, audio-related breathing rhythm and audio-related gesture.

Analysis for Headshot Data Augmentation. The row 8 in Table 2 shows that headshot data augmentation significantly impacts synchronization metrics (Sync-D, Sync-C).

Analysis for PhD Loss. We also validate the impact of each component in the PhD Loss for EchoMimicV2. As shown in rows 12 to 14 of Table 2, we observe that L_{pose} has a significant impact on overall metrics because it compensates for the incompleteness of pose condition. Additionally, L_{detail} significantly boosts performance on local quality metrics such as Sync-C, Sync-D, E-FID, HKC, and HKV. Moreover, L_{low} contributes to performance improvement in quality metrics (SSIM, PSNR).

Analysis for Straightforward Baseline. We also conducted an ablation study to validate the effectiveness of the overall APDH training strategy and PhD Loss. We trained the backbone with half-body audio and hand pose conditions, without the progressive APDH strategy and PhD Loss, as a straightforward baseline. As shown in the last row of Table 2, this baseline achieves suboptimal results due to inadequate transitions between the two conditions. These results demonstrate that the APDH and PhD Loss are important for stable training with simplified conditions.

Analysis for Hands Pose Condition. Current image and video generation methods face intrinsic challenges in generating detailed hand regions. As shown in Figure 6, even state-of-the-art text-to-image methods (*e.g.* FLUX.1) struggle with hand synthesis, an issue magnified in audio-driven generation due to the weak correlation between audio signals and motion. To address this, EchoMimicV2 combines hand pose and audio conditions, demonstrating strong hand repair capabilities despite the low proportion of hand pix-



Figure 6. High-fidelity hands generation of EchoMimicV2 when no hands or deformed hands in RefImage.

els in half-body images. Remarkably, EchoMimicV2 generates high-fidelity hands even when they are absent in the reference images as shown in Figure 6. By removing all pose conditions and maintaining other settings, we achieve a fully audio-driven animation model that captures general gestures, correlating hand rhythm with audio tones. However, this model cannot generate specific gestures like clenching fists or saluting. Due to space constraints, video results are provided in the supplementary material.

5. Limitation

This paper presents significant advancements in audio-driven half-body human animation, but it is important to acknowledge existing limitations and areas for further improvement. (1) Audio to Hand Pose Generation: The proposed method requires predefined hand pose sequences, relying on human input for high-quality animation, limiting practical applications. Future work will explore generating hand pose sequences directly from audio to in an end-to-end paradigm. (2) Animation for Non-cropped Reference Image: While EchoMimicV2 performs robustly on cropped half-body images, its performance declines on non-cropped images, such as full-body images.

6. Conclusion

In this work, we propose an effective EchoMimicV2 framework to generate striking half-body human animation driven by simplified conditions. We achieve audio-pose condition collaboration and pose condition simplification through our proposed APDH training strategy and timesteps-specific PhD Loss, while seamlessly augmenting facial expressiveness via HPA. Comprehensive experiments demonstrate that EchoMimicV2 exceeds current state-of-the-art techniques in both quantitative and qualitative results. Furthermore, we introduce a novel benchmark for evaluating half-body human animation. For the advancement of the community, we make our

source code and test dataset available for open-source use.

References

- [1] Andreas Blattmann, Tim Dockhorn, Sumith Kulal, Daniel Mendelevitch, Maciej Kilian, Dominik Lorenz, Yam Levi, Zion English, Vikram Voleti, Adam Letts, et al. Stable video diffusion: Scaling latent video diffusion models to large datasets. *arXiv preprint arXiv:2311.15127*, 2023. 1
- [2] Federica Bogo, Angjoo Kanazawa, Christoph Lassner, Peter Gehler, Javier Romero, and Michael J Black. Keep it smpl: Automatic estimation of 3d human pose and shape from a single image. In *Computer Vision—ECCV 2016: 14th European Conference, Amsterdam, The Netherlands, October 11–14, 2016, Proceedings, Part V 14*, pages 561–578. Springer, 2016. 3
- [3] Tim Brooks, Bill Peebles, Connor Holmes, Will DePue, Yufei Guo, Li Jing, David Schnurr, Joe Taylor, Troy Luhman, Eric Luhman, et al. Video generation models as world simulators, 2024. 1
- [4] Di Chang, Yichun Shi, Quankai Gao, Hongyi Xu, Jessica Fu, Guoxian Song, Qing Yan, Yizhe Zhu, Xiao Yang, and Mohammad Soleymani. Magicpose: Realistic human poses and facial expressions retargeting with identity-aware diffusion. In *Forty-first International Conference on Machine Learning*, 2023. 3
- [5] Haoxin Chen, Menghan Xia, Yingqing He, Yong Zhang, Xiaodong Cun, Shaoshu Yang, Jinbo Xing, Yaofang Liu, Qifeng Chen, Xintao Wang, et al. Videocrafter1: Open diffusion models for high-quality video generation. *arXiv preprint arXiv:2310.19512*, 2023. 1
- [6] Zhiyuan Chen, Jiajiong Cao, Zhiquan Chen, Yuming Li, and Chenguang Ma. Echomimic: Lifelike audio-driven portrait animations through editable landmark conditions. *arXiv preprint arXiv:2407.08136*, 2024. 2, 3, 5
- [7] Yu Deng, Jiaolong Yang, Sicheng Xu, Dong Chen, Yunde Jia, and Xin Tong. Accurate 3d face reconstruction with weakly-supervised learning: From single image to image set. In *Proceedings of the IEEE/CVF conference on computer vision and pattern recognition workshops*, pages 0–0, 2019. 7
- [8] Prafulla Dhariwal and Alexander Nichol. Diffusion models beat gans on image synthesis. *Advances in neural information processing systems*, 34:8780–8794, 2021. 1
- [9] Patrick Esser, Johnathan Chiu, Parmida Atighehchian, Jonathan Granskog, and Anastasis Germanidis. Structure and content-guided video synthesis with diffusion models. In *Proceedings of the IEEE/CVF International Conference on Computer Vision*, pages 7346–7356, 2023. 1
- [10] Rıza Alp Güler, Natalia Neverova, and Iasonas Kokkinos. Densepose: Dense human pose estimation in the wild. In *Proceedings of the IEEE conference on computer vision and pattern recognition*, pages 7297–7306, 2018. 3
- [11] Yuwei Guo, Ceyuan Yang, Anyi Rao, Zhengyang Liang, Yaohui Wang, Yu Qiao, Maneesh Agrawala, Dahua Lin, and Bo Dai. Animatediff: Animate your personalized text-to-image diffusion models without specific tuning. *arXiv preprint arXiv:2307.04725*, 2023. 1
- [12] Jonathan Ho, Ajay Jain, and Pieter Abbeel. Denoising diffusion probabilistic models. *Advances in neural information processing systems*, 33:6840–6851, 2020. 1
- [13] Alain Hore and Djemel Ziou. Image quality metrics: Psnr vs. ssim. In *2010 20th international conference on pattern recognition*, pages 2366–2369. IEEE, 2010. 7
- [14] Li Hu. Animate anyone: Consistent and controllable image-to-video synthesis for character animation. In *Proceedings of the IEEE/CVF Conference on Computer Vision and Pattern Recognition*, pages 8153–8163, 2024. 2, 3, 7
- [15] Johanna Karras, Aleksander Holynski, Ting-Chun Wang, and Ira Kemelmacher-Shlizerman. Dreampose: Fashion image-to-video synthesis via stable diffusion. In *2023 IEEE/CVF International Conference on Computer Vision (ICCV)*, pages 22623–22633. IEEE, 2023. 3
- [16] Diederik P Kingma. Auto-encoding variational bayes. *arXiv preprint arXiv:1312.6114*, 2013. 3
- [17] Gaojie Lin, Jianwen Jiang, Chao Liang, Tianyun Zhong, Jiaqi Yang, and Yanbo Zheng. Cyberhost: Taming audio-driven avatar diffusion model with region codebook attention. *arXiv preprint arXiv:2409.01876*, 2024. 2, 3, 7
- [18] Haiyang Liu, Xingchao Yang, Tomoya Akiyama, Yuantian Huang, Qiaoge Li, Shigeru Kuriyama, and Takafumi Takeuchi. Tango: Co-speech gesture video reenactment with hierarchical audio motion embedding and diffusion interpolation. *arXiv preprint arXiv:2410.04221*, 2024. 3
- [19] KR Prajwal, Rudrabha Mukhopadhyay, Vinay P Namboodiri, and CV Jawahar. A lip sync expert is all you need for speech to lip generation in the wild. In *Proceedings of the 28th ACM international conference on multimedia*, pages 484–492, 2020. 7
- [20] Sen Qiao, Yilin Wang, and Jian Li. Real-time human gesture grading based on openpose. In *2017 10th International Congress on Image and Signal Processing, BioMedical Engineering and Informatics (CISP-BMEI)*, pages 1–6. IEEE, 2017. 3
- [21] Robin Rombach, Andreas Blattmann, Dominik Lorenz, Patrick Esser, and Björn Ommer. High-resolution image synthesis with latent diffusion models. In *Proceedings of the IEEE/CVF conference on computer vision and pattern recognition*, pages 10684–10695, 2022. 1, 3
- [22] Ruizhi Shao, Youxin Pang, Zerong Zheng, Jingxiang Sun, and Yebin Liu. Human4dit: Free-view human video generation with 4d diffusion transformer. *arXiv preprint arXiv:2405.17405*, 2024. 3
- [23] Linrui Tian, Qi Wang, Bang Zhang, and Liefeng Bo. Emo: Emote portrait alive-generating expressive portrait videos with audio2video diffusion model under weak conditions. *arXiv preprint arXiv:2402.17485*, 2024. 3
- [24] Shuyuan Tu, Qi Dai, Zihao Zhang, Sicheng Xie, Zhi-Qi Cheng, Chong Luo, Xintong Han, Zuxuan Wu, and Yu-Gang Jiang. Motionfollower: Editing video motion via lightweight score-guided diffusion. *arXiv preprint arXiv:2405.20325*, 2024. 3

- [25] Thomas Unterthiner, Sjoerd Van Steenkiste, Karol Kurach, Raphael Marinier, Marcin Michalski, and Sylvain Gelly. Towards accurate generative models of video: A new metric & challenges. *arXiv preprint arXiv:1812.01717*, 2018. 7
- [26] Cong Wang, Kuan Tian, Jun Zhang, Yonghang Guan, Feng Luo, Fei Shen, Zhiwei Jiang, Qing Gu, Xiao Han, and Wei Yang. V-express: Conditional dropout for progressive training of portrait video generation. *arXiv preprint arXiv:2406.02511*, 2024. 2
- [27] Xiang Wang, Shiwei Zhang, Changxin Gao, Jiayu Wang, Xiaoqiang Zhou, Yingya Zhang, Luxin Yan, and Nong Sang. Unianimate: Taming unified video diffusion models for consistent human image animation. *arXiv preprint arXiv:2406.01188*, 2024. 3
- [28] Zhou Wang, Alan C Bovik, Hamid R Sheikh, and Eero P Simoncelli. Image quality assessment: from error visibility to structural similarity. *IEEE transactions on image processing*, 13(4):600–612, 2004. 7
- [29] Zhenzhi Wang, Yixuan Li, Yanhong Zeng, Youqing Fang, Yuwei Guo, Wenran Liu, Jing Tan, Kai Chen, Tianfan Xue, Bo Dai, et al. Humanvid: Demystifying training data for camera-controllable human image animation. *arXiv preprint arXiv:2407.17438*, 2024. 6
- [30] Huawei Wei, Zejun Yang, and Zhisheng Wang. Aniportrait: Audio-driven synthesis of photorealistic portrait animation. *arXiv preprint arXiv:2403.17694*, 2024. 2, 3
- [31] Mingwang Xu, Hui Li, Qingkun Su, Hanlin Shang, Liwei Zhang, Ce Liu, Jingdong Wang, Yao Yao, and Siyu Zhu. Hallo: Hierarchical audio-driven visual synthesis for portrait image animation. *arXiv preprint arXiv:2406.08801*, 2024. 2, 3
- [32] Zhongcong Xu, Jianfeng Zhang, Jun Hao Liew, Hanshu Yan, Jia-Wei Liu, Chenxu Zhang, Jiashi Feng, and Mike Zheng Shou. Magicanimate: Temporally consistent human image animation using diffusion model. In *Proceedings of the IEEE/CVF Conference on Computer Vision and Pattern Recognition*, pages 1481–1490, 2024. 3
- [33] Shuai Yang, Yifan Zhou, Ziwei Liu, and Chen Change Loy. Rerender a video: Zero-shot text-guided video-to-video translation. In *SIGGRAPH Asia 2023 Conference Papers*, pages 1–11, 2023. 1
- [34] Shurong Yang, Huadong Li, Juhao Wu, Minhao Jing, Linze Li, Renhe Ji, Jiajun Liang, Haoqiang Fan, and Jin Wang. Megactor- σ : Unlocking flexible mixed-modal control in portrait animation with diffusion transformer. *arXiv preprint arXiv:2408.14975*, 2024. 3
- [35] Zhendong Yang, Ailing Zeng, Chun Yuan, and Yu Li. Effective whole-body pose estimation with two-stages distillation. In *Proceedings of the IEEE/CVF International Conference on Computer Vision*, pages 4210–4220, 2023. 3
- [36] Lvmin Zhang, Anyi Rao, and Maneesh Agrawala. Adding conditional control to text-to-image diffusion models. In *Proceedings of the IEEE/CVF International Conference on Computer Vision*, pages 3836–3847, 2023. 3, 5
- [37] Wenxuan Zhang, Xiaodong Cun, Xuan Wang, Yong Zhang, Xi Shen, Yu Guo, Ying Shan, and Fei Wang. Sadtalker: Learning realistic 3d motion coefficients for stylized audio-driven single image talking face animation. In *Proceedings of the IEEE/CVF Conference on Computer Vision and Pattern Recognition*, pages 8652–8661, 2023. 2, 3
- [38] Yuang Zhang, Jiayi Gu, Li-Wen Wang, Han Wang, Junqi Cheng, Yuefeng Zhu, and Fangyuan Zou. Mimi-motion: High-quality human motion video generation with confidence-aware pose guidance. *arXiv preprint arXiv:2406.19680*, 2024. 2, 3, 7
- [39] Shaobin Zhuang, Kunchang Li, Xinyuan Chen, Yaohui Wang, Ziwei Liu, Yu Qiao, and Yali Wang. Vlogger: Make your dream a vlog. In *Proceedings of the IEEE/CVF Conference on Computer Vision and Pattern Recognition*, pages 8806–8817, 2024. 3, 7